CHAPTER 6

Dielectric Properties of Modified $BiFeO_3$ Ceramics

In this work, the pure and modified $BiFeO_3$ (BFO) ceramics (BFO doped with Sb) were synthetical by a solid-state reaction method. Phase formation, microstructure, and dielectric properties were investigated. The samples showed a main phase of rhombohedral BFO. The additive inhibited grain growth, with average grain size decreasing from ~14 μm for pure BFO to 3μm for the modified BFO samples. The dielectric constant of the modified samples tended to improve with the additive. This improvement can be related a conduction mechanism in the studied samples

6.1 Introduction

Multiferroic materials which combine two or more properties of ferroelectric, ferromagnetism, and ferroelasticity are gaining much attention due to their physical properties as well as possibility of practical electronic applications [1-7]. $BiFeO_3$ (BFO) is one of such materials and has a rhombohedrally distorted simple perovskite structure (ABO_3). It exhibits an antiferromagnetic behavior with a relatively high Neel temperature (T_N ~370 ˚C) and ferroelectric behavior with a high Curie temperature (T_C ~830 ˚C) [7]. This material has been fabricated in many forms such as single crystal, ceramics and thin films [2-5]. The properties the fabricated BFO have also been intensively investigated for many years past. However, it should be noted that most BFO ceramics exhibits week ferroelectric behavior. Furthermore, BFO ceramics also present a large leakage current, which hampered its practical applications. The existence of Fe^{2+} ions and oxygen vacancies has been proposed as a reason for the large leakage current [8]. In order to improve the properties of BFO, several techniques have been proposed such as processing, forming some solid solutions between BFO and other

ลิขสิทธิ์มหาวิทยาลัยเชียงใหม่
Copyright© by Chiang Mai University
All rights reserved

materials, and doping with some elements [1-2]. In case doping, several elements such as Ba, Ca, Ce, La, Nb, Pb and Mn have been introduced into BFO lattices [1-2, 9-13]. However, electrical properties of BFO doped with Sb have not been investigated, to our knowledge. In the present work, we report for our results showing the effects of Sb doping on the properties of BFO ceramics.

6.2 Experimental

$BiFeO_3$ doped with Sb was synthesized by a solid-state reaction. Bi_2O_3 (Aldrich, 99.0% purity), Fe_2O_3 (Aldrich, 99.0% purity) and Sb_2O_5 (Aldrich, 99.9% purity) were used as raw metal oxide materials. The raw materials were weighed and then suspended in ethanol and intimately mixed in a ball milling machine for 24 h using zirconia balls as a grinding media. After drying for 24 h, the dried powder was ground, sieved and then calcined at 800 ^oC for 2 h. The obtained mixture was dried and then uniaxially pressed into a disc shape with a diameter of 1.5 cm. Excess Bi_2O_3 (3 wt. %) was introduced prior to powder calcination to compensate for any Bi_2O_3 that may have been lost from the powder due to volatilization at high temperature. The green discs were sintered at 850 ^oC with a dwell time of 2 h. The density of the sintered samples was determined by Archimedes' principle. Phase formation of the samples was examined by X-ray diffraction (XRD) technique. For electrical measurement, the sintered samples were polished to obtain parallel surfaces and silver paste electrodes were applied to make an electrode. The dielectric properties of the pellet ceramics were measured using a LCR meter.

ลิขสิทธิ์มหาวิทยาลัยเชียงใหม่
Copyright© by Chiang Mai University
All rights reserved

6.3 Results and discussion

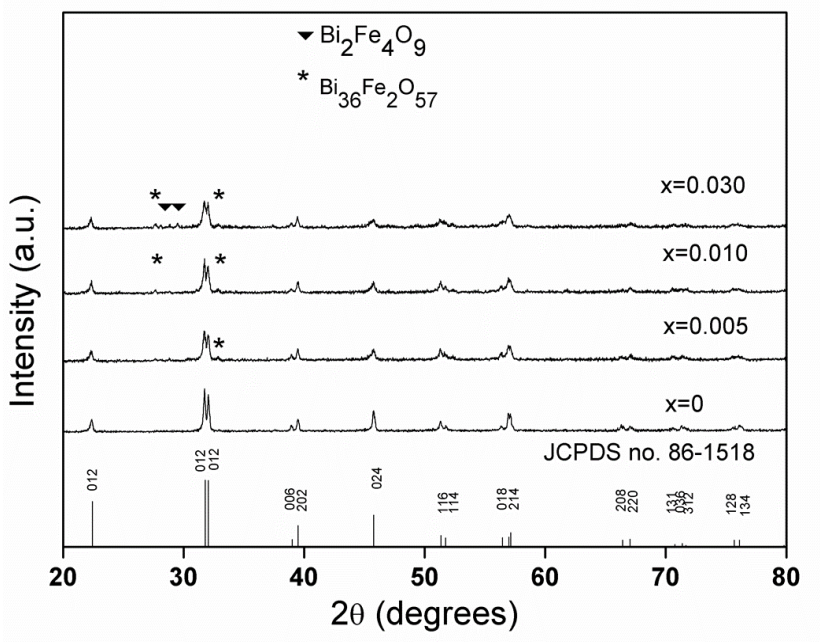

Figure 6.1 displays the XRD patterns of pure and modified BFO ceramics

The XRD result indicates that all main diffraction peaks correspond to a perovskite phase of BFO according to JCPDS file no. 86-1518. In case the unmodified sample, the XRD data shows a pure phase of BFO. The obtained result agrees with the work done by Jim et al. [7]. After doping, however, peaks of impurity phases are presented as seen and indicated in Fig 1. These second phase were identified as $Bi_2Fe_4O_9$ and $Bi_{36}Fe_2O_{57}$ according to JCPDS file no. 25-0090 and 42-0181, respectively. The appearance of the impurity phases implies that the additive inhibits the formation of BFO phase. However, the slightly shift in XRD peaks suggests that small amount of Sb ions have entered into the BFO lattices. To check this possibility, energy band gap of the studied ceramics was determined by a UV-Visible spectrometer. The energy band gaps of the samples are listed in Table 6.1. The energy band gap values of the studied samples are in a range of 2.595- 2.579 eV. Plot of absorption spectrum as wavelength of the $BiFeO_3$ ceramics had showed in Figure 6.6-6.9. The energy band gap range in the present work is close to that reported in previous work [14]. The slightly change in energy band gap therefore confirms the XRD investigation. Furthermore, it should be noted that the XRD peaks

ลิขสิทธิ์มหาวิทยาลัยเชียงใหม่
Copyright© by Chiang Mai University
All rights reserved

become broader and their intensity decrease with increasing Sb concentration. This implies that the modified BFO ceramics exhibits a lower degree of crystallinity.

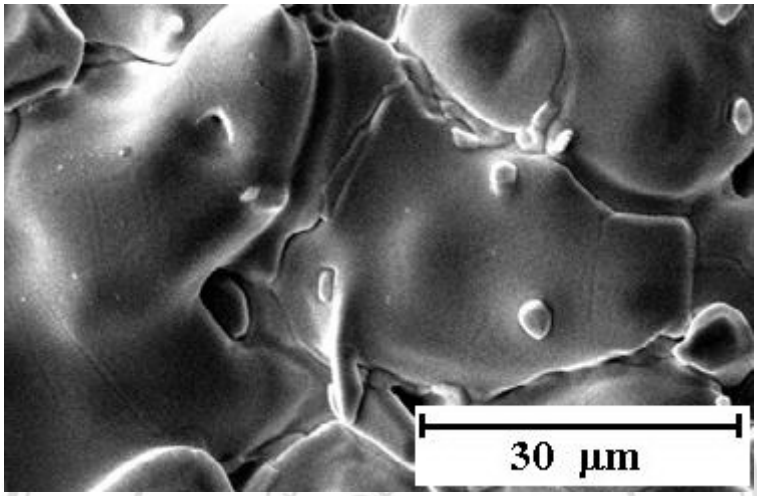

Figure 6.2 SEM micrographs of pure BFO ceramic.

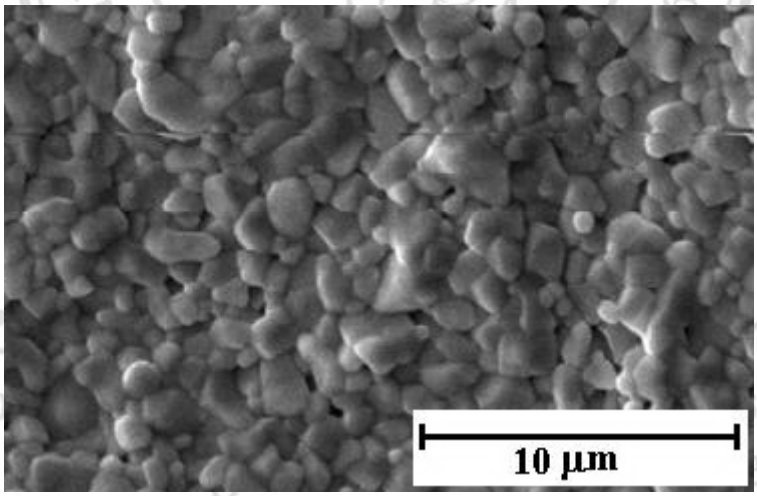

Figure 6.3 SEM micrographs of modified BFO ceramics with x=0.005.

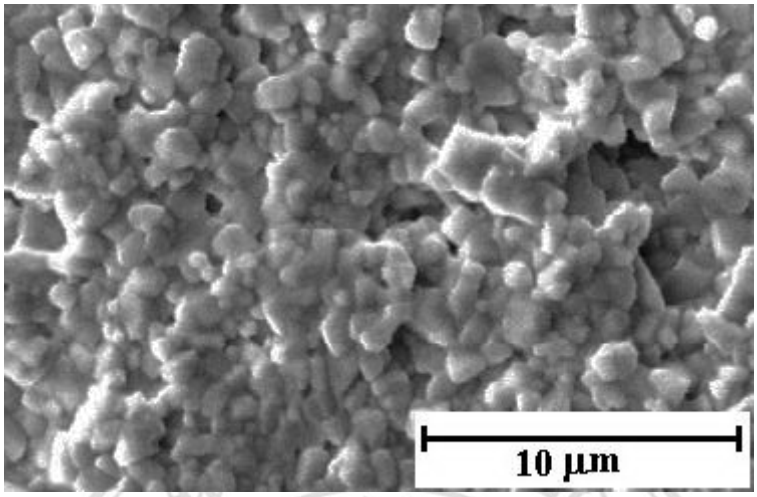

Figure 6.4 SEM micrographs of pure and modified BFO ceramics with x=0.010.

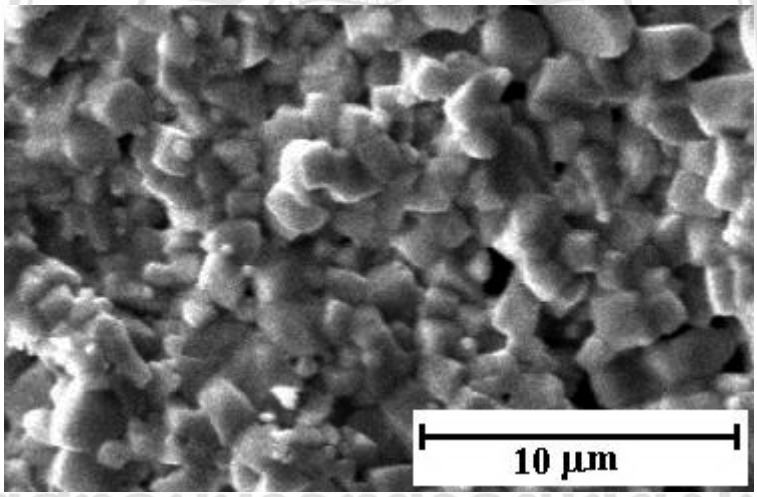

Figure 6.5 SEM micrographs of pure and modified BFO ceramics with x=0.030.

ลิขสิทธิ์มหาวิทยาลัยเชียงใหม่
Copyright© by Chiang Mai University
All rights reserved

The SEM micrographs of the selected ceramic surfaces are illustrated in Fig. 6.2-6.5. It can be seen that small amount of Sb additive produces a large change in grain size. Average values of grain size, sharply decreases from ~14 μm for the pure BFO ceramic to ~3 μm for the x = 0.005 ceramic and then slightly changes with further Sb concentrations.This result suggestes that Sb doping not only inhibites the BFO phase formation but also suppress the grain growth. The impurity phases may be form at the

grain boundaries and prevent grain boundary movement during the sintering process as a result in forming of fine grains in the modified samples.

TABLE 6.1. Energy band gab (E_g) and activation energy (E_a) of the studied ceramics.

Sb concentration (x)	**E_g (eV)**	**E_a(eV)**
0.000	2.5950	0.7520
0.005	2.5850	0.7718
0.010	2.5790	0.7908
0.030	2.5790	0.9412

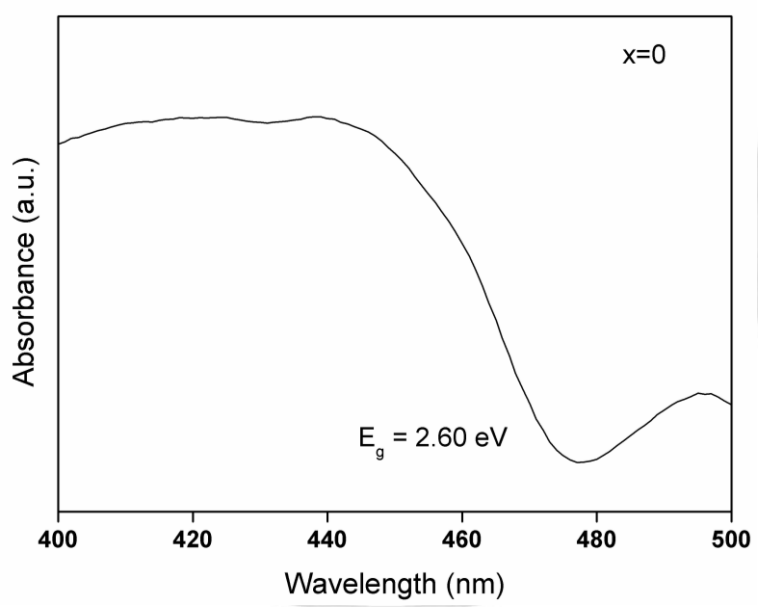

Figure 6.6 UV–Vis absorption spectrum of the $BiFeO_3$ when x=0.000.

ลิขสิทธิ์มหาวิทยาลัยเชียงใหม่
Copyright© by Chiang Mai University
All rights reserved

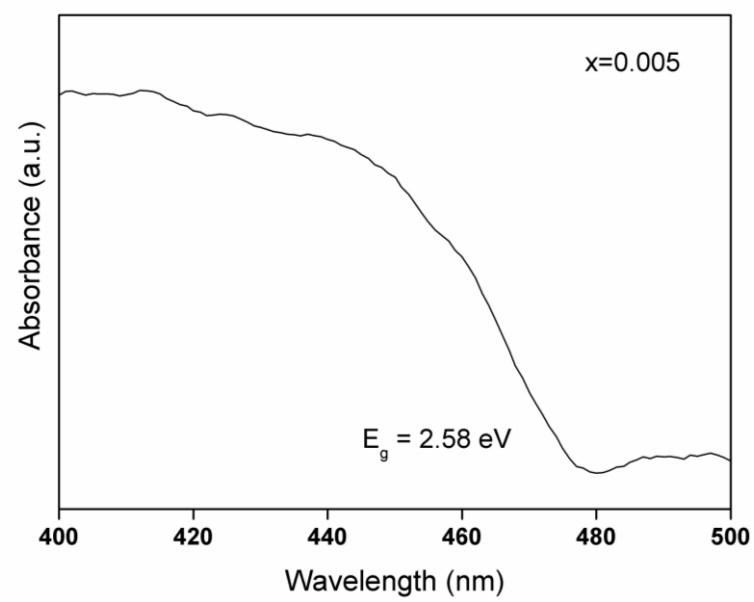

Figure 6.7 UV–Vis absorption spectrum of the $BiFeO_3$ when x=0.005.

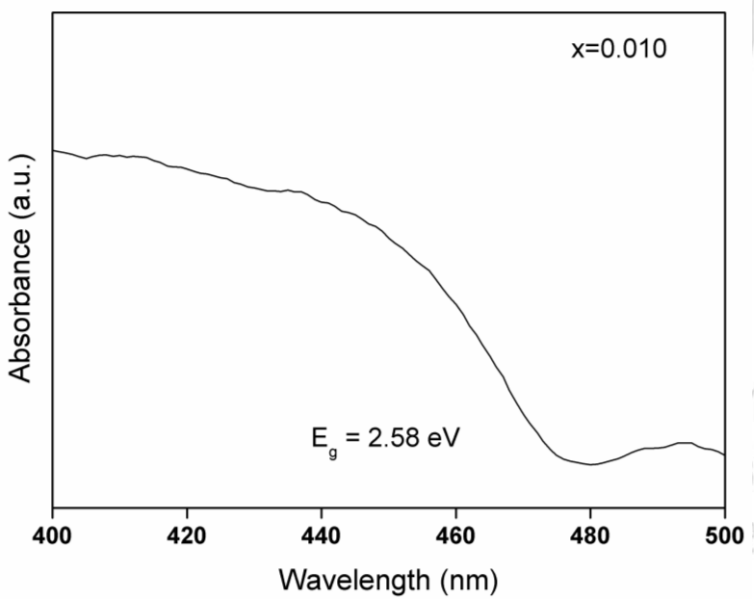

Figure 6.8 UV–Vis absorption spectrum of the $BiFeO_3$ when x=0.010.

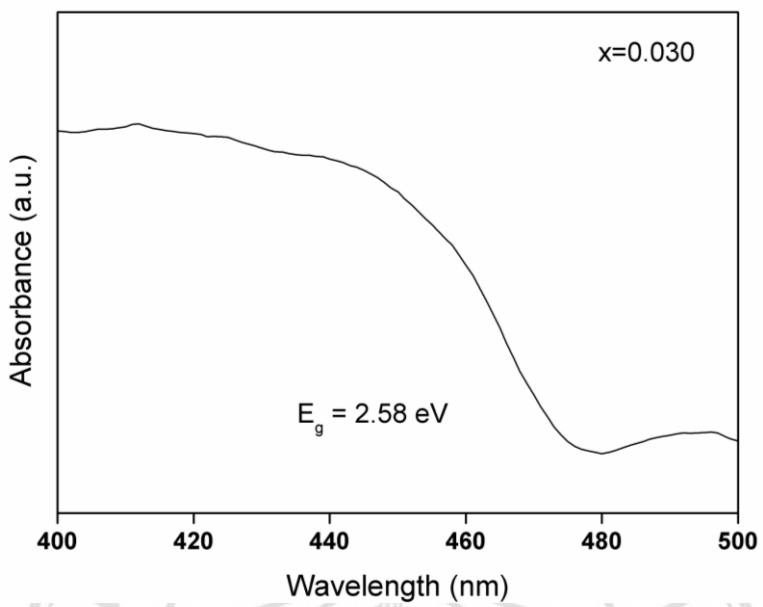

Figure 6.9 UV–Vis absorption spectrum of the $BiFeO_3$ when x=0.030.

ลิขสิทธิ์มหาวิทยาลัยเชียงใหม่
Copyright© by Chiang Mai University
All rights reserved

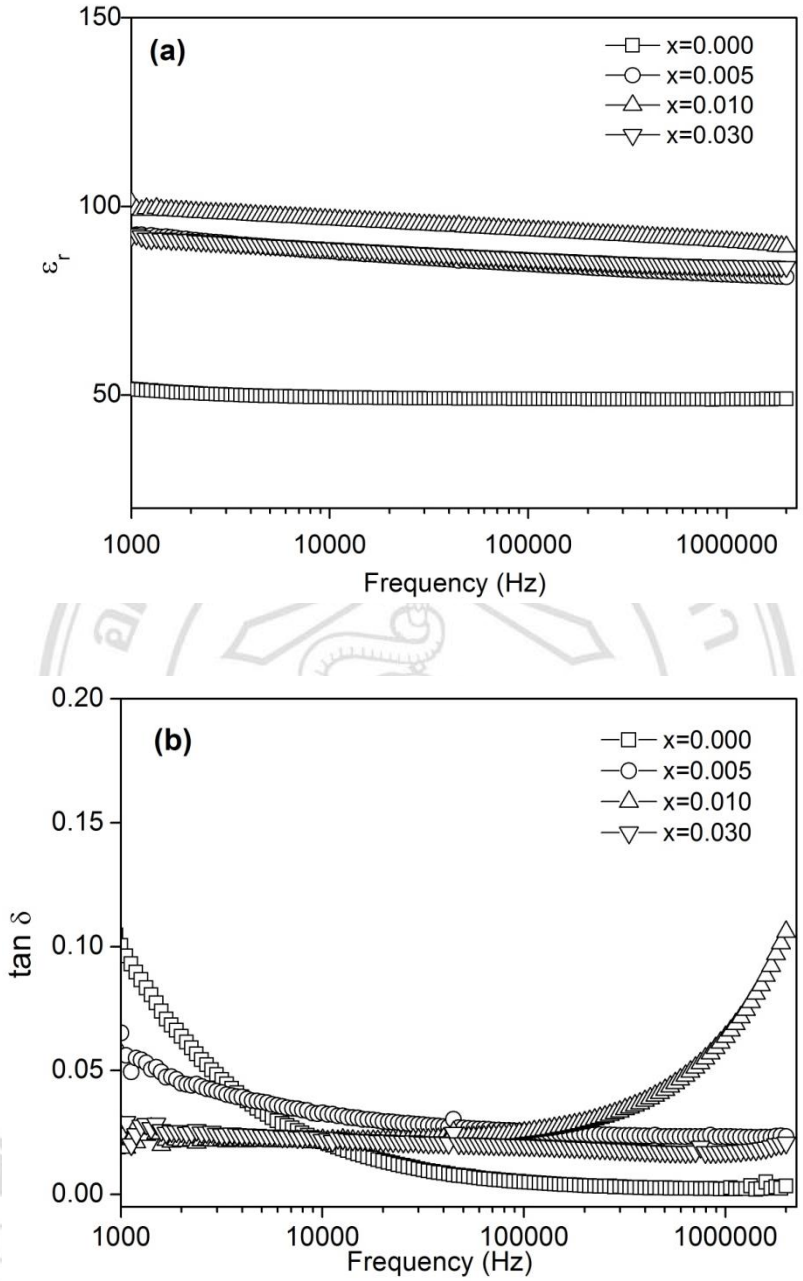

Figure 6.10 (a) Dielectric constant (ε_r) and (b) loss tangent (tan δ) as a function of frequency (at room temperature).

The dielectric constant and loss tangent as a function of frequency at room temperature is shown in Fig.6.10. General trend indicates that all samples exhibtes a dielectric frequency stability, i.e. dielectric constant and loss tangent of all samples slightly change with increasing frequency. In case the pure BFO ceramics, the dielectric

ลิขสิทธิ์มหาวิทยาลัยเชียงใหม่
Copyright© by Chiang Mai University
All rights reserved

constant at 10 kHz is ~50. This value is consistent with many previous works [15]. After doping, an enhancement in dielectric constant is noted. The dielectric constants of modfiled cereamics are in a range of 88-97, but the 0.010 samples shows the maximum dielectric constant. In addition, the loss tantgent values of all ceramics are lower than 0.04.

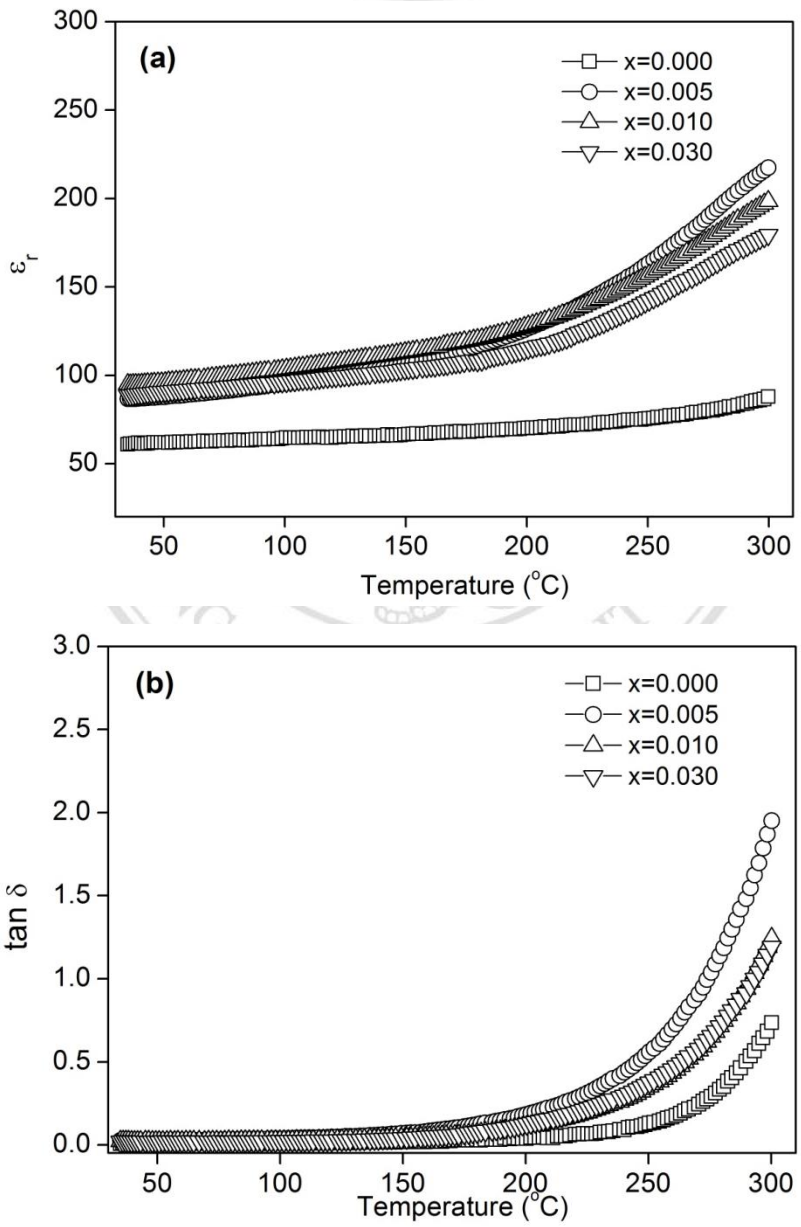

Figure 6.11 XRD patterns of BFO sintered ceramics.

The temperature dependence of the dielectric properties of the studied ceramics at 10 kHz is shown in the Fig.6.11. All samples presented an increase in dielectric constant and loss tangent with the temperature. The increase in dielectric constant and loss tangent with increasing temperature can be related to the thermally induced enhancement of the conductivity contribution [16]. It should be noted that Sb doping also produces an enhancment in the dielectric constant thougth the measured temperature.

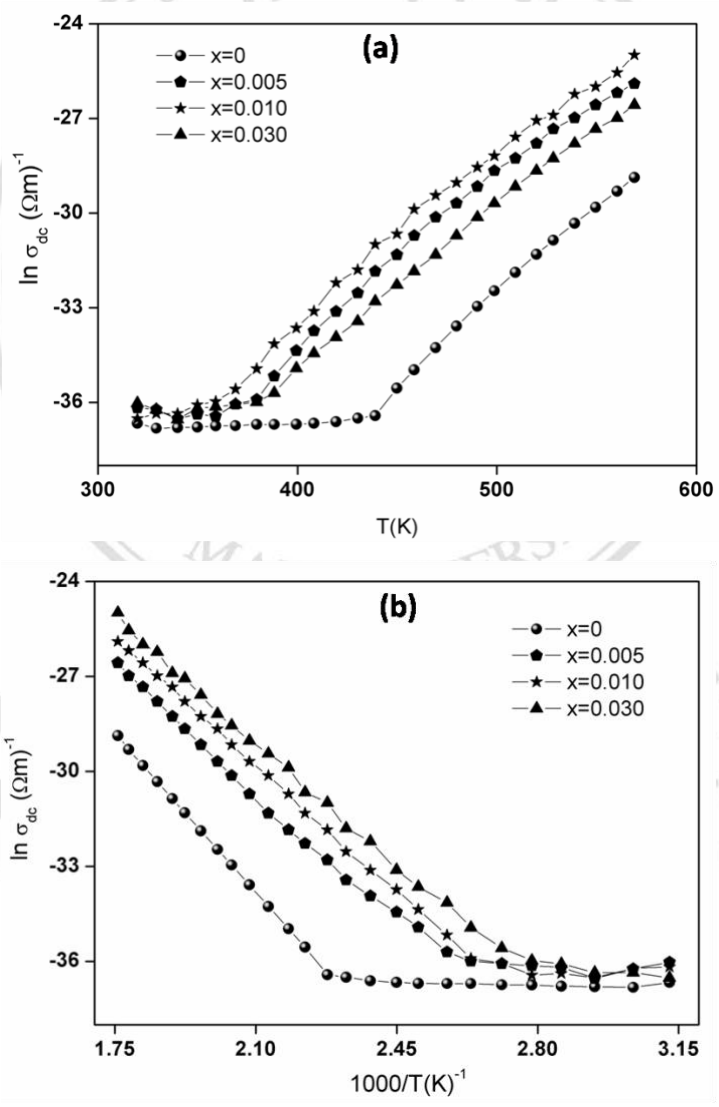

Figure 6.12 (a) dc-conductivity versus Temperature and (b) Arrhenius plots for the ceramics.

To check the conduction mechanism at high temperature. Conductivity (dc) as a function of temperature was performed. Fig.6.12(a) presents plots of dc conductivity versus temperature of the studied ceramics. The activation energy (Ea) was also calcuted from this data by means of fitting an Arrhenius plots as seen in Fig.6.12(b). The activation energy values are in a range of 0.75-0.94 eV (Table 1). Therefore, conduction mechanism at high temperature can be related to oxygen vacancy conduction (E_a=0.89 eV).

To investestigate the effect of Sb doping on the electrical properties in more detail, a techinque of impedance spectroscopy was used in this work. Fig. 6.13 shows complex impedance planes measured at room temperature. In this work, all plots show only part of a semi-circle, with the centre lying below the Z'-axis. This character is simmilar to previous works [17-18] Therefore, a parallel combination of a resistor (R) and capacitor (C) is used to model conduction processes in this work [17-18]. The unmodified sample has bigger arc than that of the modified samples. This indicates a higer resistance the unmodified samples, i.e. the addition of Sb_2O_3 could reduced the resistivity of the modified ceramics. Thus, the enhancement in dielectric constant of the modified samples can be linked with conduction mechanism in the ceramics.

ลิขสิทธิ์มหาวิทยาลัยเชียงใหม่
Copyright© by Chiang Mai University
All rights reserved

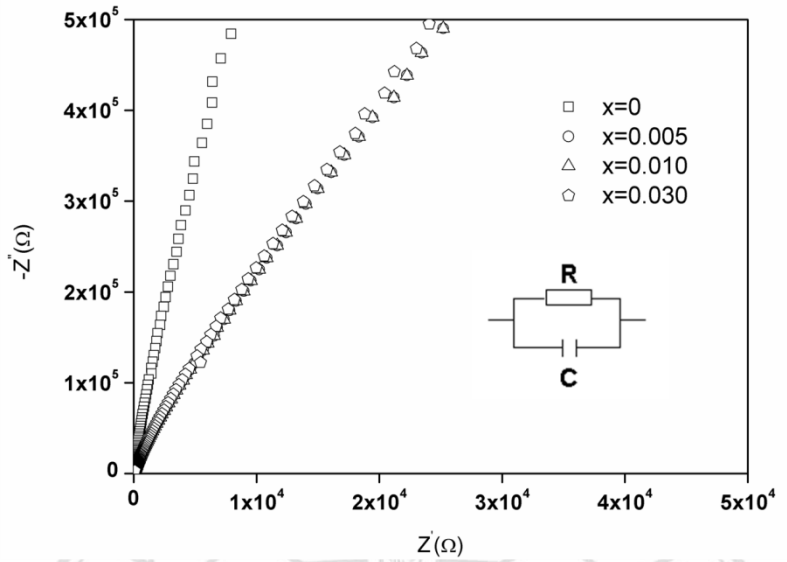

Figure 6.13 Nyquist plots of the impedance (Z' and Z") the pure BFO and modified BFO ceramics. Inset show the equivalent circuit.

6.4 Conclusion

Phase formation, microstructure, and dielectric properties of the pure and Sb doped BFO ceramics were determined. Main phase of the studied ceramics is BFO. The obtained data also indicates that small amount of Sb ions have entered into the BFO lattices. A large change in grain size after doping, suggested that the additive suppresses grain growth. Addition of the additive also results the enhancement in dielectric constant which can be linked with oxygen vacancy conduction.

ลิขสิทธิ์มหาวิทยาลัยเชียงใหม่
Copyright© by Chiang Mai University
All rights reserved

6.5 Reference

[1] T. Kimura, S. Kawamoto, I. Yamada, M. Azuma, M. Takano and Y. Tokura, "Magnetocapacitance effect in multiferroic $BiMnO_3$," Physical Review Letters, Vol. 67, 2003, Page 18401.

[2] W.M. Zhu and Z.G. Ye, "Effects of chemical modification on the electrical properties of $0.67BiFeO_3$-$0.33PbTiO_3$ ferroelectric ceramics," Ceramics International, Vol. 30, pp. 1435-1442, 2004.

[3] G. Cheng, M. Xiangjian, S. Jinglan, M. Jianhua, L. Tie and C. Junhao, "Ferroelectric Properties of $BiFeO_3$ thin films prepared via a simple chemical solution deposition," Ferroelectrics, Vol. 406, 2010, Page 137-142.

[4] Y. H. Chu, L. W. Martin, Q. Zhan, P. L. Yang, M. P. Cruz, K. Lee, M. Barry, S. Y. Yang and R. Ramesh, "Epitaxial multiferroic $BiFeO_3$ thin films: progress and future directions," Ferroelectrics, Vol. 354, 2007. Page 167-177.

[5] J. Wang, J.B. Neaton, H. Zheng, V. Nagarajan, S.B. Ogale, B. Liu, D. Viehland, V. Vaithyanathan, D.G. Schlom, U.V. Waghmare, N.A. Spaldin, K.M. Rabe, M. Wuttig, and R. Ramesh, "Epitaxial $BiFeO_3$ multiferroic thin film heterostructures," Science, Vol. 299, 2003, Page 1719-1722.

[6] J. B. Neaton, C. Ederer, U. V. Waghmare, N. A. Spaldin, and K. M . Rabe, "First-principles study of spontaneous polarization in multiferroic $BiFeO_3$," Physical Review Letters, Vol. 71, Page 014113.

[7] J. K. Kim, S. S. Kim and W. J. Kim, "Sol-gel synthesis and properties of multiferroic $BiFeO_3$," Materials Letters, Vol. 59, 2005, Page 4006-4009.

[8] C. Wang, M. Takahashi, H. Fujino, X. Zhao and E. Kume, "Leakage current of multiferroic $(Bi_{0.6}Tb_{0.3}La_{0.1})FeO_3$ thin films grown at various oxygen pressures by pulsed laser deposition and annealing effect," Journal of Applied Physics, Vol. 99, 2006, Page 054104.

[9] R. Das and K. Mandal, "Magnetic, ferroelectric and magnetoelectric properties of Ba-doped BiFeO3," Journal of Magnetism and Magnetic Materials, Vol. 324, 2012, Page 1913-1918.

[10] S.K. Pradhan and B.K. Roul, "Electrical behavior of high resistivity Ce-doped $BiFeO_3$ multiferroic," Physica B, Vol. 407, 2012, Page 2527-2532.

ลิขสิทธิ์มหาวิทยาลัยเชียงใหม่
Copyright© by Chiang Mai University
All rights reserved

[11] K. Ahadi, A. Nemati, S. M. Mahdavi, “Conductor–insulator transition and electronic structure of Ca-doped $BiFeO_3$ films,” Materials Letters, Vol. 83, 2012, Page 124-126.

[12] C. F. Chung, J. P. Lin and J. M. Wu, “Influence of Mn and Nb dopants on electric properties of chemical-solution-deposited $BiFeO_3$ films,” Applied Physics Letters, 2006, Page 242909.

[13] F. G. Garciaa, C.S. Riccardi and A.Z. Simõesa, “Lanthanum doped $BiFeO_3$ powders: Syntheses and characterization,” Journal of Alloys and Compounds, Vol. 501, 2010, Page. 25-29.

[14] A.Kumar, R. C. Rai, N. J. Podraza, S. Denev,1 M. Ramirez, Y. Chu, L. W. Martin, J. Ihlefeld, T. Heeg, J. Schubert, D.G. Schlom, J. Orenstein, R. Ramesh, R. W. Collins, J. L. Musfeldt, and V. Gopalan, “Linear and nonlinear optical properties of $BiFeO_3$,” Applied Physics Letters, Vol. 92, 2008, Page 121915.

[15] M. M. Kumar, V. R. Palkar, K. Srinivas and S. V. Suryanarayana, “Ferroelectricity in a pure $BiFeO_3$ ceramic,” Applied Physics Letters, Vol. 76, 2000, Page 2764-2766.

[16] V. A. Khomchenko, D. A. Kiselev, M. Kopcewicz, M. Maglione, V. V. Shvartsman, P. Borisov, W. Kleemann, A. M. L. Lopes, Y. G. Pogorelov, J. P. Araujo, R. M. Rubinger, N. A. Sobolev, J. M. Vieira, A. L. Kholkin, “Doping strategies for increased performance in $BiFeO_3$,“ Journal of Magnetism and Magnetic Materials, Vol. 321, 2009, Page 1692-1698.

[17] A. J. Bell, T. Schlegel, M. Alduraibil, M. A. Khan,T. P. Comyn and J. Rodel, “Impedance Spectroscopy of Mn-Doped $BiFeO_3$-$PbTiO_3$ Ceramics,” Application of ferroelectrics, 2006.

[18] Y. Lin, H. Yang, Z. Zhu, “Impedance spectroscopy analysis of $0.7BiFeO_3$-$0.3BaTiO_3/BiY_2Fe_5O_{12}$ compositeswith simultaneously improved magnetization and remnant polarization,“ Materials Chemistry and Physics, Vol. 136, 2012, Page 286-291.

ลิขสิทธิ์มหาวิทยาลัยเชียงใหม่
Copyright© by Chiang Mai University
All rights reserved